Critical role of the neutrophil-associated high-affinity receptor for IgE in the pathogenesis of experimental cerebral malaria

Adeline Porcherie,[1] Cedric Mathieu,[1] Roger Peronet,[1] Elke Schneider,[2] Julien Claver,[3,4] Pierre-Henri Commere,[5] Hélène Kiefer-Biasizzo,[5] Hajime Karasuyama,[6] Geneviève Milon,[7] Michel Dy,[2] Jean-Pierre Kinet,[8] Jacques Louis,[1] Ulrich Blank,[3,4] and Salaheddine Mécheri[1]

[1]Institut Pasteur, Unité de Biologie des Interactions Hôte Parasites, F-75015 Paris, France
[2]Centre National de la Recherche Scientifique, UMR 8147, Université Paris Descartes, 75743 Paris, France
[3]Institut National de la Santé et de la Recherche Médicale U699, F-75018 Paris, France
[4]UMR-S699, Faculté de Médecine Paris Diderot - Site Xavier Bichat, Université Paris Diderot-Paris 7, F-75018 Paris, France
[5]Institut Pasteur, Imagopole, F-75015 Paris, France
[6]Department of Immune Regulation and JST, Core Research for Evolutional Science and Technology, Tokyo Medical and Dental University Graduate School, Tokyo 113-8549 Japan
[7]Institut Pasteur, Unité d'Immunophysiologie et Parasitisme Intracellulaire, F-75015 Paris, France
[8]Department of Pathology, Beth Israel Deaconess Medical Center, Boston, MA 02215

The role of the IgE–FcεRI complex in malaria severity in *Plasmodium falciparum*–hosting patients is unknown. We demonstrate that mice genetically deficient for the high-affinity receptor for IgE (FcεRIα-KO) or for IgE (IgE-KO) are less susceptible to experimental cerebral malaria (ECM) after infection with *Plasmodium berghei* (*Pb*ANKA). Mast cells and basophils, which are the classical IgE-expressing effector cells, are not involved in disease as mast cell–deficient and basophil-depleted mice developed a disease similar to wild-type mice. However, we show the emergence of an FcεRI$^+$ neutrophil population, which is not observed in mice hosting a non–ECM-inducing *Pb*NK65 parasite strain. Depletion of this FcεRI$^+$ neutrophil population prevents ECM, whereas transfer of this population into FcεRIα-KO mice restores ECM susceptibility. FcεRI$^+$ neutrophils preferentially home to the brain and induce elevated levels of proinflammatory cytokines. These data define a new pathogenic mechanism of ECM and implicate an FcεRI-expressing neutrophil subpopulation in malaria disease severity.

CORRESPONDENCE
Salaheddine Mécheri:
smecheri@pasteur.fr

Abbreviations used: BMMC, BM-derived mast cell; ECM, experimental cerebral malaria; iRBC, infected RBC; MC, mast cell; *Pb*ANKA, *Plasmodium berghei* ANKA; TLR, Toll-like receptor.

Clinical malaria is associated with high levels of circulating cytokines (Kwiatkowski et al., 1990). Although balanced production of IFN-γ, TNF, IL-1, and IL-6 is capable of controlling parasite growth (Stevenson and Riley, 2004), their excessive production exacerbates disease severity (Grau and de Kossodo, 1994; Kwiatkowski, 1995) and contributes to the development of cerebral malaria (Grau et al., 1989; Kwiatkowski et al., 1990).

The inflammatory effector mechanisms remain ill-defined and complex. They involve innate immune responses through members of the mammalian Toll-like receptor (TLR) family that recognize parasite molecules (Coban et al., 2007), or hemozoin, which is a digestion product of hemoglobin (Coban et al., 2005). Antibody-mediated inflammatory responses may also be critical. Although the role of IgG subclasses has been characterized in some detail (Shi et al., 1996; Metzger et al., 2003), the functional implication of IgE antibodies in malaria pathogenesis needs to be clarified. Past studies have shown that patients with severe malaria show higher IgE levels against *P. falciparum* than those with uncomplicated malaria (Perlmann et al., 1994, 2000). Other studies reported a reduced risk of severe malaria (Bereczky et al., 2004) and protection from cerebral malaria of IgE antibodies (Nacher et al., 2000). IgE bind to high-affinity

Supplemental material can be found at:
http://doi.org/10.1084/jem.20110845

IgE receptors (FcεRI) on mast cells (MCs) and basophils, as well as to low-affinity IgE receptors (FcεRII/CD23) on B cells, granulocytes, and many other cell types. Interaction of CD23 with IgE immune complexes activates iNOS gene transcription leading to nitric oxide production, which is thought to cause cerebral malaria (Maneerat et al., 2000). Activation of basophils (Nyakeriga et al., 2003) and MCs (Furuta et al., 2006) that express FcεRI, but not CD23, may also exacerbate malaria pathogenesis through histamine secretion. High plasma and tissue histamine levels increased disease severity in humans infected with *P. falciparum* and in several animal models of *Plasmodium* infection (Srichaikul et al., 1976; Bhattacharya et al., 1988). Histidine decarboxylase KO mice exhibited a marked resistance to severe malaria induced by *Plasmodium berghei* ANKA, an effect that involved binding to H1 and H2 receptors (Beghdadi et al., 2008).

To examine the role of IgE/FcεRI-mediated inflammatory processes in malaria pathogenesis, we studied mice that were genetically deficient for FcεRIα (Dombrowicz et al., 1993b) and IgE (Oettgen et al., 1994) after inoculation of *Pb*ANKA. The present investigations document that both mouse populations are resistant to ECM and control parasite development. Neither MCs nor basophils home to the brain, but a subset of FcεRI$^+$ neutrophils that were otherwise shown to emerge in the BM of *Pb*ANKA-hosting mice do home to the brain, disrupting its steady-state features.

RESULTS

FcεRI and IgE deficiency confers protection against ECM

To examine whether IgE synthesis and FcεRI-expressing cells are involved in ECM, we infected FcεRIα-KO mice that are resistant to IgE-mediated anaphylaxis (Dombrowicz et al., 1993b) with *Pb*ANKA via mosquito bites. The majority (80%) of *Pb*ANKA-infected WT mice died from ECM within 7–12 d (median survival, day 8; Fig. 1 b), whereas 90% of FcεRIα-KO mice survived at day 15 and did not develop ECM. Mice that resisted ECM later died of parasitemia-induced anemia without neurological signs (median survival: day 27; Fig. 1 b). Parasitemia increased over time similarly in C57BL/6 WT and FcεRIα-KO mice until day 15 after infection (Fig. 1 a). After day 15, parasitemia in WT mice that had survived ECM continued to rise, whereas in FcεRIα-KO mice it reached a plateau, indicating that, in contrast to WT mice, they were able to control parasite growth at later stages of infection. Quantitative RT-PCR analysis in brains of WT mice also showed an increase in FcεRIα mRNA over time until day 6, when it became significant, paralleling the appearance of the first signs of ECM (Fig. 1 c).

MC numbers in peritoneum and BM showed no difference between FcεRIα-KO and WT mice, ruling out any defect in MC development and function in FcεRIα-KO mice (Fig. S1 a; Dombrowicz et al., 1993b). Because histamine was previously implicated in malaria pathogenesis (Beghdadi et al., 2008), we measured histamine contents in BM cells and peritoneal MCs and found no differences between the two genotypes (Fig. S1 b). Additionally, plasma histamine levels were similar in FcεRI-KO mice and WT mice (Fig. S1 c).

ECM resistance in the absence of FcεRIα likely reflects a role of IgE in malaria pathogenesis, as this receptor serves as a signaling relay after ligand binding (Bryce et al., 2004) and after antigen-specific cross-linking of IgE-sensitized cells (Blank and Rivera, 2004). In concordance, IgE-KO mice were less susceptible to ECM after infection with *Pb*ANKA. They survived >3 wk with 60% not developing ECM,

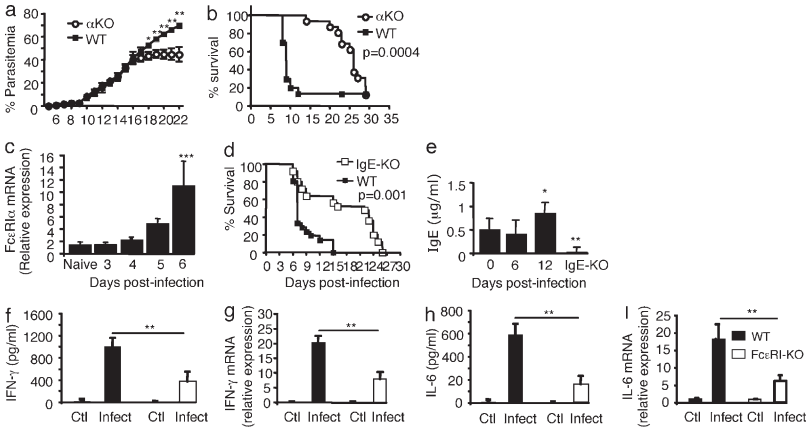

Figure 1. FcεRI expression and IgE are critical for the pathogenesis of ECM. FcεRIα-KO mice and C57BL/6N (WT) mice were infected with *Pb*ANKA through mosquito bites (8–10 mosquitoes per mouse). (a) Parasitemia (Mann-Whitney test; *, $P < 0.036$; **, $P < 0.008$). (b) Kaplan-Meier survival plots (log-rank test, $n = 52$, $P = 0.0004$). Data are from five independent experiments. (c) C57BL/6N (WT) mice were sacrificed at indicated time points after receiving blood-stage parasites of *Pb*ANKA inoculated intraperitoneally (10^6 infected RBCs), and brain tissues were prepared for mRNA extraction. Transcription of the α chain of FcεRI was evaluated by real-time RT-PCR. mRNA expression was normalized to hypoxanthine phosphoribosyltransferase expression. ***, ANOVA, $P = 0.0055$; followed by an a posteriori Fisher's PLSD test, $P = 0.0008$. Results were from two independent experiments. (d–i) IgE-KO ($n = 25$) and C57BL/6N (WT; $n = 21$) mice were infected with *Pb*ANKA through intraperitoneal inoculation of blood-stage parasites (10^6 infected RBCs). (d) Kaplan-Meier survival plots were recorded (log-rank test, $P = 0.035$). Survival data are from four independent experiments. (e) Total IgE as measured in the plasma from noninfected (d0) and *Pb*ANKA-infected mice taken at indicated time points. Background value determinations of IgE were performed in sera from IgE-KO mice. * and ** indicate that differences are significant (Mann-Whitney test, $n = 5–7$, $0.01 < P < 0.05$ and $0.001 < P < 0.01$, respectively) relative to the basal level. Results are from three independent experiments. (f–i) Serum levels of IFN-γ (f) and IL-6 (h) were quantified by ELISA at day 6 after infection. Transcription of IFN-γ (g) and IL-6 (i) in the brain ($n > 6$/group) 6 d after infection as evaluated by real-time RT-PCR. Gene mRNA expression is normalized to the endogenous control gene GAPDH, and the relative expression levels were calculated using the uninfected animals as a calibrator. Data are presented as the means ± SD from two independent experiments. **, $P < 0.02$.

whereas 75% of WT controls died of ECM (Fig. 1 d). Together, these data suggest that IgE-mediated signaling via FcεRI is essential for the occurrence of ECM. Considering the role of IgE, we found that total plasma IgE levels became significantly elevated only at day 12 after infection, as measured in surviving WT mice (Fig. 1 e).

In agreement with reports that ECM pathology in *Pb*ANKA-infected mice is associated with increased pro-inflammatory IFN-γ (Hunt and Grau, 2003) and IL-6 production (Lou et al., 1998), significantly higher levels were found in plasma and brain tissue of ECM-sensitive C57BL/6 mice than in FcεRIα-KO mice (Fig. 1, f–i). These data demonstrate that IgE and FcεRIα deficiency confers resistance to ECM and that the absence of signaling-competent receptors results in lower inflammatory cytokines in plasma and brain tissue.

Neither MCs nor basophils contribute to the development of ECM

To investigate the role of FcεRI-expressing cells, we first used MC-deficient W^{sh}/W^{sh}, which, like the previously used FcεRIα-KO and IgE-KO mice, are on the C57BL/6 background. MC-deficient W^{sh}/W^{sh} and WT mice were infected with *Pb*ANKA strain via mosquito bites. Parasitemia over time (Fig. 2 a) and survival rates (Fig. 2 b) showed no significant differences between both mouse strains excluding a role of MCs as major pathological effectors. To confirm this, FcεRIα-KO and W^{sh}/W^{sh} mice were reconstituted with WT MCs yielding an average of 1.2 and 1.05% $FcεRI^+$ WT MCs, respectively, in the peritoneal fluid 10 wk after reconstitution, as compared with 1.75% in WT animals (Fig. S1 d). No effect was seen in reconstituted W^{sh}/W^{sh} mice and reconstituted FcεRIα−KO mice remained resistant to ECM (Fig. S1 e). These data formally rule out MCs as the cellular IgE targets in malaria pathogenesis.

Alternative FcεRI-expressing cells are basophils. To investigate their implication, mice were treated with the basophil-depleting antibody Ba103 1 d before infection. Severe depletion of $DX5^+/FcεRI^+$ blood basophils (Fig. S2) did not improve disease susceptibility as compared with control mice and the survival rates were not significantly different compared with FcεRIα-KO or IgE-KO mice (compare Fig. 1, b and d, and Fig. 2 c). Collectively, these data suggest that $FcεRI^+$ cells other than MCs and basophils play a pivotal role in ECM development.

Similar infection outcomes were obtained whether mice were infected via mosquito bites or via infected RBCs (iRBCs). Henceforth, mice were infected via iRBCs.

In mice, expression of the FcεRI is thought to be limited to MCs and basophils. However, it has been reported recently that FcεRIα and γ polypeptides are expressed in rat and mouse pinealocytes, the melatonin-secreting cell of the pineal gland (Ganguly et al., 2007). As the brain is a target tissue in ECM, we speculated that FcεRI expressed by pinealocytes contribute to disease expression. To address this, adoptive transfer experiments were performed by injecting BM cells from FcεRIα-KO and C57BL/6 mice into irradiated FcεRIα-KO mice. Only mice that received $FcεRI^+$ BM cells developed ECM (Fig. 2 d), ruling out a significant contribution of pinealocytes in disease expression. Conversely, reconstitution of irradiated C57BL/6 mice with BM from syngeneic mice or from FcεRIα-KO mice showed that only the latter acquired resistance to ECM (unpublished data). Altogether, these data demonstrate that the FcεRIα-expressing cells that contribute to disease expression are of hematopoietic origin.

To exclude functional overlap between MCs and basophils, it was important to test the effect of depleting basophils in the mast cell–deficient Wsh mice. Preliminary data show that depletion of basophils in mast cell–deficient mice did not alter the phenotype of infected mice in regard to the development of ECM (unpublished data), suggesting that both cell lineages are apparently not involved in CM pathogenesis. Given the reported binding of IgE to FcγRIV and the major role of FcγRIV in neutrophil activation (Hirano et al., 2007; Mancardi et al., 2008), it was necessary to preclude any possibility of this receptor to contribute to the observed effects associated with the FcεRI. To this end, C57BL/6 mice were inoculated with *Pb*ANKA-infected erythrocytes, and then treated with 200 µg of anti-FcγRIV mAb (9e9 antibody) every other day from day 2 to day 6 after infection. Binding of the

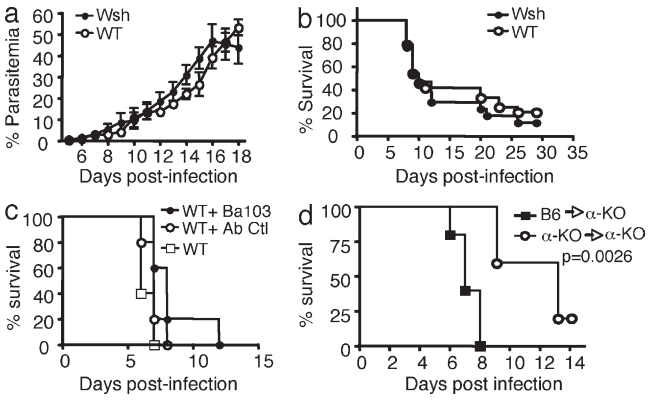

Figure 2. Mast cells and basophils are not involved in malaria pathogenesis. Mast cell–deficient W^{sh}/W^{sh} and C57BL/6N (WT) mice were infected with *Pb*ANKA through mosquito bites (8–10 mosquitoes per mouse). Parasitemia (a) and Kaplan-Meier survival plots (b) were recorded (log-rank test; $n = 32$ of each genotype; $P = 0.1$). There were no significant differences in parasitemia between groups. Data are from four independent experiments. (c) C57BL/6N mice were treated with basophil-depleting BA103 antibody 1 d before *Pb*ANKA inoculation. Untreated, BA103-treated C57BL/6N, and control antibody-treated (Ab-Ctl) C57BL/6N mice were infected via mosquito bites. Kaplan-Meier survival plots were recorded (log-rank test; $n = 11$ of each genotype; $P = 0.0179$). Median mortality is 5 d for the two control groups, and 7 d for BA103-treated C57BL/6N mice. Data shown are from two independent experiments. (d) After irradiation, FcεRIα-KO mice intravenously received 5×10^6 BM cells isolated either from FcεRIα-KO mice or from WT C57BL/6N mice. The two groups of mice were infected with *Pb*ANKA with 10^6 *Pb*ANKA-iRBC. Kaplan-Meier survival plots were recorded (log-rank test; $n = 12$ of each genotype; $P = 0.0026$). Data shown are from two independent experiments.

antibody was assessed throughout the infection period, as shown by FACS analysis of blood leukocytes gated on $CD45^+$ cells (preliminary results; unpublished data). Occurrences of ECM and survival data were strictly similar between mice that received the anti-FcγRIV antibody or the isotype control antibody (preliminary results; unpublished data).

Identification of neutrophils and eosinophils as novel FcεRI-expressing cells induced during malaria disease

In search of FcεRI-expressing cells, we surmised that neutrophils and eosinophils might represent inflammatory cells, which under the particular circumstance of *Plasmodium* infection, could express FcεRI and cause the disease. A kinetic analysis of the frequency of $7/4^+$ $Ly6G^+$ neutrophils, $Siglec\text{-}F^+$ eosinophils, and $Fc\varepsilon RI^+$ cells among blood leukocytes showed that neutrophils increased constantly over time, whereas eosinophils remained stable at around 5% (Fig. 3 a). The proportion of total $Fc\varepsilon RI^+$ cells also increased steadily (Fig. 3 a). The most highly represented $Fc\varepsilon RI^+$ cells among examined blood leukocytes were neutrophils reaching up to 6% (Fig. 3 b). $Fc\varepsilon RI^+$ eosinophils peaked at day 4 rising from 0.2 to 4% and then decreased between d6-8 reaching 1.5% (Fig. 3 b).

In the BM, the proportion of neutrophils and eosinophils decreased from day 0 to 4, and then slightly increased until day 8 for neutrophils, while eosinophils decreased again after a short rise (Fig. 3 c). Fig. 3 d shows that naive mice expressed a small but detectable proportion of $Fc\varepsilon RI^+$ neutrophils (1.8%) and eosinophils (1.9%). This proportion peaked at 8.5 and 6% for neutrophils and eosinophils, respectively, at day 4 after infection, whereas at day 6 and 8 after infection, the fraction of $Fc\varepsilon RI^+$ cells declined for the two cell types. In parallel, basophils increased from 0.5% at day 0 to 2% at day 8, whereas the fraction of MCs remained unchanged.

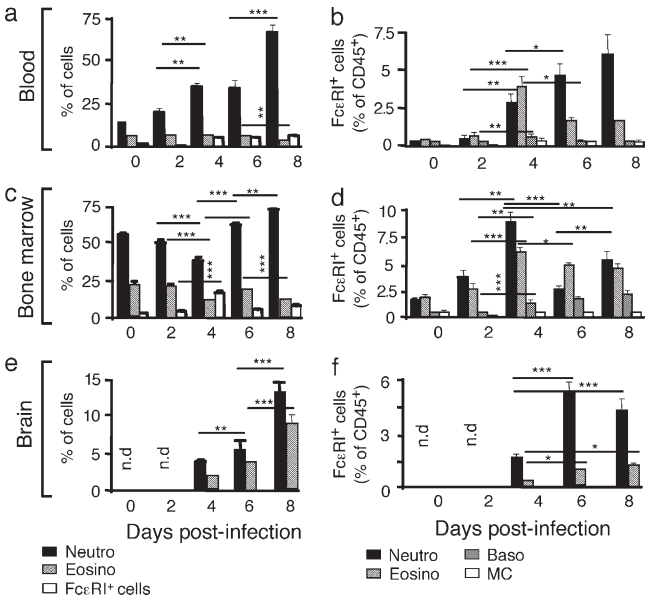

Figure 3. Induction of $Fc\varepsilon RI^+$ neutrophils and eosinophils during *Plasmodium* infection. WT C57BL/6N mice were inoculated with 10^6 *Pb*ANKA-iRBC. At indicated time points after inoculation, blood cells (a and b), BM cells (c and d), and brain tissue (e and f) were analyzed for the presence of total neutrophils, eosinophils, and $Fc\varepsilon RI\alpha^+$ leukocytes (a, c, and e), as well as for $Fc\varepsilon RI\alpha^+$ neutrophils, basophils, eosinophils, and mast cells, as indicated (b, d, and f). Values represent the means ± SD. Significant differences are indicated (ANOVA, followed by an a posteriori Fisher's PLSD test; ***, $P < 0.001$; **, $P < 0.02$; *, $P < 0.05$). Data are from two independent experiments.

In the brain, no cells were detected until 4 d after infection, which is when both neutrophils (4.9%) and eosinophils (2.3%) appeared, and their proportions reached 14 and 9%, respectively, at 8 d after infection (Fig. 3 e). The proportions of $Fc\varepsilon RI^+$ neutrophils and eosinophils were, however, strikingly different with an accumulation of ∼5% of neutrophils at 6–8 d, as compared with 1.3% of $Fc\varepsilon RI^+$ eosinophils (Fig. 3 f). It must be noted that neither mast cells nor basophils were present at any given time (Fig. 3, e and f). An illustration of a FACS analysis of neutrophil populations associated with brain tissue taken at 6 d after infection and showing ECM signs is shown in Fig. 4. Double labeling of leukocyte populations with anti-7/4 and anti-Ly6G antibodies revealed a highly enriched proportion of $Fc\varepsilon RI^+$ $7/4^+$ $Ly6G^+$ neutrophils (55–61%) associated with brain tissue of mice showing ECM signs at 6 d after infection (Fig. 4, top). To verify whether the increase in receptor expression occurs in the neutrophil population present in the brain, and also to determine whether this increase in expression only occurs in mouse strains susceptible to CM when infected with *Pb*ANKA, mice infected with the non–ECM-inducing *Pb*NK65 parasites did not show any sequestration of $Fc\varepsilon RI^+$ neutrophils in their brain even at 20 d after infection (Fig. 4, bottom). It must also be emphasized that there were small amounts of leukocytes associated with the brain tissue. Indeed, the $CD45^+$ population in the brain of *Pb*NK65-infected mice represents only 0.25% of total cells, whereas the same population was 20-fold higher (5%) in *Pb*ANKA-infected mice.

Collectively, these data show that a significant proportion of neutrophils and eosinophils expressed FcεRI during infection with *Pb*ANKA parasite.

Depletion of neutrophils protects mice from ECM

For depletion experiments, we used the NIPM-R14 mAb, in which staining patterns shows a complete overlap between the anti-Ly6G and the 7/4 antibodies. Administration of 200 µg of the antineutrophil mAb NIMP-R14 1 d before infection, which elicited complete depletion of neutrophils up to day 6 (unpublished data), prevented the development of neurological signs of ECM, and protected mice from death as compared with those treated with control IgG isotype (Fig. 5 a). Death occurred on average between day 20–25, without neurological signs from hyperparasitemia-induced anemia (median survival time, 21 d versus 7 d for neutrophil-depleted and control mice, respectively; $n = 8$; $P = 0.006$), with no significant difference in final parasitemia ($P > 0.05$; Fig. 5 b).

To examine the possible contribution of eosinophils to ECM pathogenesis, C57BL/6 mice were treated with eosinophil-depleting anti–mouse Siglec-F antibody 1 d before infection and

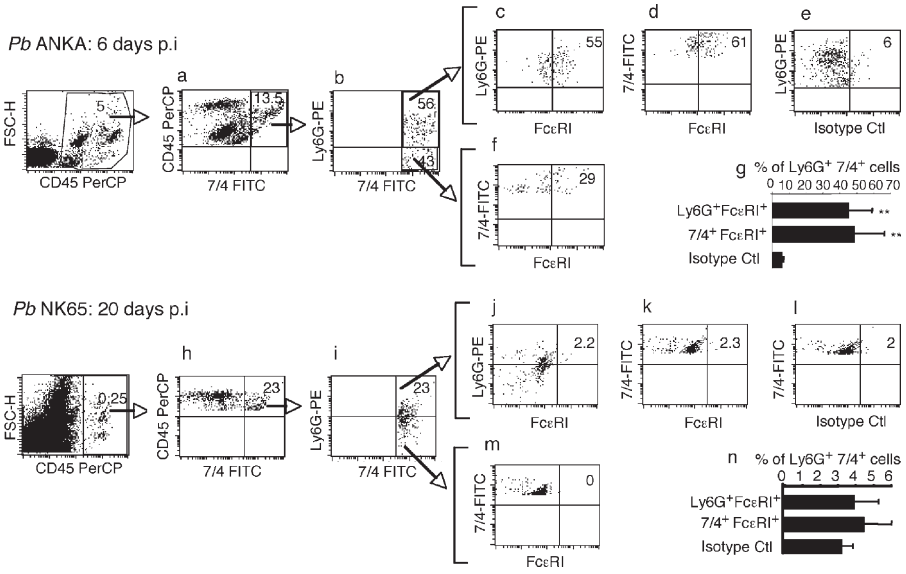

Figure 4. Selective sequestration of FcεRI+ neutrophils in the brain of mice infected with *Pb*ANKA. C57BL/6 mice were infected with the ECM-inducing *Pb*ANKA (top) or with the ECM noninducing *Pb*NK65 (bottom). At day 6 and 20 after infection, respectively, they were perfused and brains were collected. Isolated cells were labeled with anti–CD45-PerCP, 7/4-FITC, Ly6G-PE, and FcεRI-APC. (a and h) Cells gated on $CD45^+$-$7/4^+$. (b and i) $7/4^+$-$Ly6G^+$ neutrophils. A population of neutrophils expressing FcεRI is shown in c and d, as compared to cells labeled with an isotype control antibody (e). A subpopulation of $7/4^+$-$Ly6G^+$ cells was also positive for FcεRI (f). Similar analysis for mice infected with the *Pb*NK65 parasite strain was performed (j, k, l, and m). Quantitative analysis of $Ly6G^+$-$7/4^+$-FcεRI+ neutrophil populations was performed on five individual *Pb*ANKA-infected mice (g) and on *Pb*NK65-infected mice (n). ** indicates significant differences as compared with control IgG ($n = 5$; $P < 0.007$). Results were obtained from two independent experiments.

at day 4 after infection. No significant differences between eosinophil-depleted and control IgG-treated mice were observed in the development of ECM (Fig. 5 c) and parasitemia (Fig. 5 d). These data demonstrate that neutrophils, but not eosinophils, play a critical role in the pathogenesis of ECM and that cell depletion does not directly affect parasitemia.

To establish if neutrophil depletion was equally effective after infection, we performed a kinetic analysis. Mice were treated before infection or at day 4, 5, or 6 after infection with anti–neutrophil-depleting antibody. Treatment at 4 d after infection was equally effective as depletion 1 d before infection (Fig.5, a and e). Treatment on day 5 after infection was less protective, although significant ($n = 12$; $P = 0.031$; Fig. 5 f) compared with mice treated on day 6 after infection ($n = 12$; $P = 0.074$), which is when mice started to develop the first signs of ECM (Fig. 5 g). Thus, late depletion of neutrophils is no longer protective once the pathogenetic processes are established, particularly in the brain, where on day 5 these events are already in place (Beghdadi et al., 2008).

To analyze the role of $FcεRI^+$ neutrophils in the initiation of ECM pathology, FcεRIα-KO mice were repleted with BM-derived $FcεRI^+$ neutrophils from *Pb*ANKA-infected C57BL/6 mice 6 d after infection. $FcεRI^+$ cells were enriched in the low-density layers of Percoll gradient (50–45% and <45%; Fig. S3) before FACS sorting. Double-positive cells gated on 7/4 and Ly6G expression gave rise to two neutrophil populations: $Ly6G^+$ $7/4^+$ $FcεRI^+$ neutrophils (9.3%) and $Ly6G^+$ $7/4^+$ $FcεRI^-$ neutrophils. 90.7% were obtained from *Pb*ANKA-infected mice, whereas in normal mice the $Ly6G^+$ $7/4^+$ $FcεRI^+$ neutrophil population represents only 1% (Fig. S4, b and c). Additional morphological analysis of $FcεRI^+$ and $FcεRI^-$ neutrophil populations showed that they were phenotypically indistinguishable, as shown by cytospin analysis (Fig. S4, d and e). Sorted triple-positive ($Ly6G^+$ $7/4^+$ $FcεRI^+$) neutrophils or double-positive ($Ly6G^+$ $7/4^+$ $FcεRI^-$) neutrophils were injected intravenously into recipient FcεRIα-KO mice. Before injection, these cells were analyzed for their possible contamination with other leukocytes, and as shown in Fig. S4 f, sorted cells consisted of highly pure neutrophil populations with only minor contamination from $Siglec\text{-}F^+$ cells, $CD11c^+$ cells, and $F4/80^+$ cells. FcεRIα-KO mice repleted with $Ly6G^+$ $7/4^+$ $FcεRI^+$ neutrophils acquired susceptibility to ECM, as compared with those reconstituted with $FcεRI^-$ neutrophils ($n = 15$, $P = 0.0087$; Fig. 5 h). To analyze brain localization, naive or infected FcεRIα-KO or WT C57BL/6 mice (6 d after infection) were injected intravenously with 10^6 CFSE-labeled sorted neutrophils ($7/4^+$ $Ly6G^+$ $FcεRI^+$) obtained from infected C57BL/6 mice. As shown in Fig. 5 i, a significant proportion of CFSE-labeled neutrophils was found to be associated to brain tissue of both infected recipient FcεRIα-KO (4.9%) and WT C57BL/6 mice (4.5%) compared with noninfected FcεRIα-KO (0.7%) and WT C57BL/6 mice (0.6%), respectively. Similar results were obtained 1 and 24 h after injection, suggesting that $7/4^+$ $Ly6G^+$ $FcεRI^+$ home rapidly and stably to the brain tissue of infected mice. These data demonstrate that the expression of $FcεRI^+$ in neutrophils is critical for the development of ECM.

Biochemical characterization of FcεRI expressed by neutrophils

As neutrophils ordinarily do not express FcεRI, we further characterized this receptor in cells from *Pb*ANKA-infected mice. Highly homogeneous double-positive $Ly6G^+$ $7/4^+$ cells obtained by FACS sorting (Fig. S4), subjected to analysis using RT-PCR, showed that neutrophils from naive mice expressed low levels of FcεRIα mRNA and expression increased in infected mice (Fig. 6 a). Flow cytometry confirmed that naive mice expressed only low levels of surface FcεRI and IgE-binding (~1%). On day 6 after infection, ~9–10% of neutrophils stained positive with anti-FcεRIα and anti-IgE, indicating that they were IgE-sensitized (Fig. 6 b). CD23,

another receptor, which may also account for IgE binding, was not expressed by neutrophils from naive or infected mice (Fig. 6 b). Confocal image analysis also confirmed that FcεRIα was colocalized with the FcεRIγ subunit (Fig. 6 c), whereas FcεRIβ was undetectable (not depicted). Immunoblot analysis of cell lysates confirmed the presence of FcεRIγ and the absence of FcεRIβ, whereas FcεRIβ was readily detected in RBL-2H3 and BMMC lysates (Fig. 6 d). To exclude the possibility that the lack of the FcεRI β chain is caused by a proteolytic degradation, presence of the β chain was assessed at the transcriptional level. Analysis of neutrophils by real time qPCR clearly indicate that sorted FcεRI$^+$ neutrophils express the α chain, whereas the β chain is not present (unpublished data). Neutrophils, whether obtained from naive or infected mice also expressed FcγRIV (Fig. 6 b). Although FcγRIV has been reported to bind IgE^b (Hirano et al., 2007) or both IgE^a and IgE^b allotypes (Mancardi et al., 2008) at high concentrations, we did not detect IgE^b-binding under steady-state conditions in naive mice, and IgE-binding could not be blocked with anti-FcγRIV antibody in cells from infected mice (unpublished data). We also performed coimmunoprecipitation experiments to analyze the subunit composition of FcεRI. The receptor was directly immunoprecipitated with IgE-Sepharose to avoid precipitation of murine IgG receptors through protein G from purified neutrophils, which may contain cell-bound IgG. Co-immunoprecipitation of receptor under mild conditions (0.3% Triton X-100) revealed the specific presence of FcεRIγ, whereas FcεRIβ was absent. Both β and γ chains were readily coimmunoprecipitated from BMMC lysates (Fig. 6 e). The γ chain was also immunoprecipitated in the presence of anti-FcγRIV blocking antibody (unpublished data) excluding that coimmunoprecipitation of the γ chain was caused by FcγRIV. Together, these data indicated that the parasite-induced neutrophil population expressed an unconventional FcεRI in the absence of FcεRI β chain. To assess the functionality of this receptor, neutrophils were passively sensitized with anti-DNP–specific IgE mAb. Stimulation of sensitized cells for 4 h with DNP-HSA elicited significant amounts of TNF and IL-6 release (Fig. 6 f).

DISCUSSION

In this work, we report the implication of molecular and cellular components of the IgE-mediated allergic inflammatory cascade in malaria pathogenesis. Using a murine model of ECM, we show that the inflammatory response elicited by IgE–FcεRI complexes drives development of ECM. This did not involve MCs or basophils. A major finding was that *Pb*ANKA-induced expression of FcεRI in neutrophils

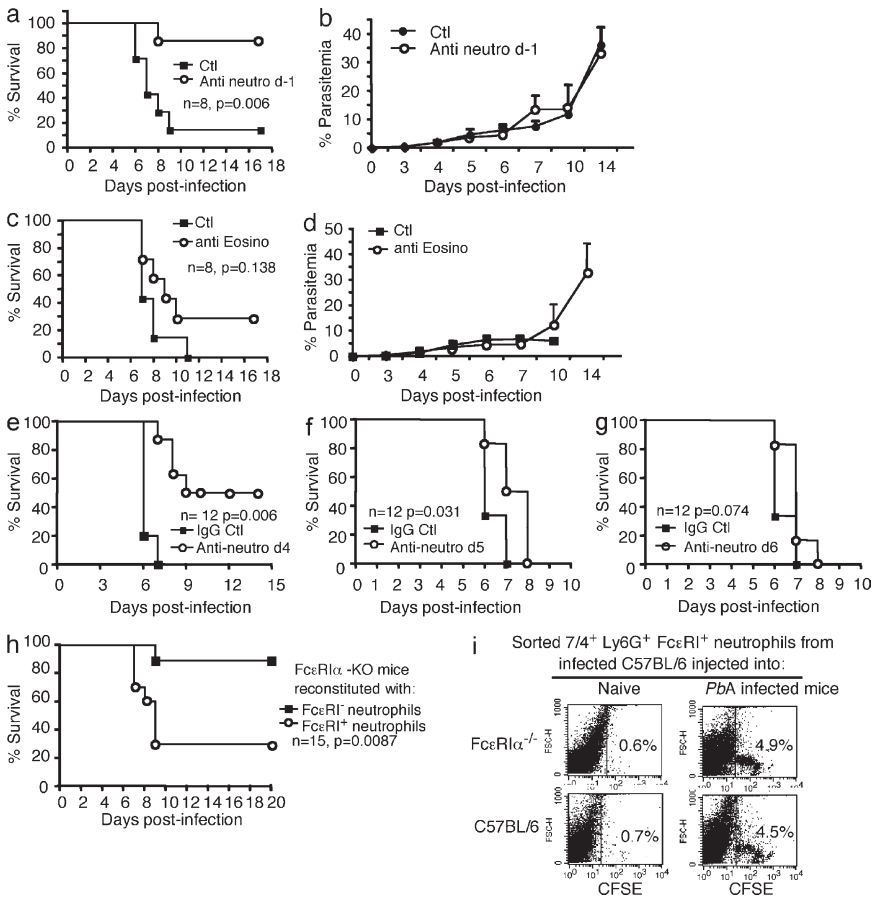

Figure 5. FcεRI$^+$ neutrophils play a critical role in malaria pathogenesis. C57BL/6N mice were treated (n = 8) or not (n = 8) with 200 µg of anti-neutrophil (NIMP-R14) antibodies (a and b) or 100 µg of antieosinophil (anti–Siglec-F; c and d) 1 d before inoculation with 10^6 *Pb*ANKA-iRBC. The anti–Siglec-F–treated group received a second injection of antibody at day 4. Kaplan-Meier survival plots (a and c) and parasitemia (b and d) were recorded (log-rank test; P = 0.138). Data were obtained from three independent experiments. (e–g) Time-dependent effect of neutrophil depletion on mouse survival during ECM. C57BL/6 mice (n = 12) inoculated with 10^6 *Pb*ANKA-infected RBCs were treated with control IgG antibody or with the anti-neutrophil antibody NIM-PR14 (200 µg/mouse) for 4 (e), 5 (f), or 6 d (g) after infection. Kaplan-Meier survival plots were recorded using (log-rank test). Data shown are from two independent experiments. (h) Reconstitution of FcεRIα-KO mice with FcεRIα$^+$ or FcεRI$^-$ neutrophils. At day 6 after inoculation with 10^6 iRBCs, FcεRIα-KO mice received 5 × 10^6 Ly6G$^+$ 7/4$^+$ FcεRI$^+$ or Ly6G$^+$ 7/4$^+$ FcεRI$^-$ neutrophils from infected C57BL/6 mice (Fig. S4). Kaplan-Meier survival plots were recorded (n = 15; P = 0.0087). Data shown are representative of two independent experiments. (i) Sequestration of CFSE-labeled FcεRI$^+$ neutrophils in the brain of infected recipient mice: Naive or infected FcεRIα-KO or WT C57BL/6 mice (day 6 after infection with 10^6 *Pb*ANKA-infected erythrocytes) were injected intravenously with 10^6 CFSE-labeled sorted neutrophils (Ly6G$^+$ 7/4$^+$ FcεRI$^+$) obtained from infected C57BL/6 mice. Leukocytes were prepared, 1 or 24 h after injection, from brains of PBS-perfused recipient mice. These data are representative of three different mice in each group.

and eosinophils and that depletion of neutrophils, but not eosinophils, had a positive clinical outcome.

In humans, studies aiming at establishing the allergic nature of malaria disease report conflicting results ranging from disease-aggravating to disease-protecting roles of IgE (Perlmann et al., 1997; Bereczky et al., 2004). To clarify this issue, we used genetically deficient animals or antibody-depleted cell populations to examine crucial components of the allergic inflammatory response in malaria pathogenesis. We found that targeted disruption of IgE or the α chain of FcεRI led to resistance to the development of ECM after infection with *Pb*ANKA. These results indicate a pathological role of IgE that acts via FcεRI to promote disease development. Interestingly, FcεRI-α-KO mice showed a more marked resistant phenotype than IgE-KO mice, leaving open the possibility for additional disease-aggravating signaling events via FcεRI. This may include galectin 3, an alternative ligand for FcεRI. In agreement, deletion of the galectin-3 gene in susceptible C57BL/6 mice resulted in partial protection from ECM (Oakley et al., 2009). In both FcεRI-α-KO and IgE-KO mice, the observed clinical immunity occurred in the absence of antiparasite immunity. The association of FcεRI with the neuropathological disorders observed during ECM was further emphasized by the constant increase of the receptor α chain expression in the brain

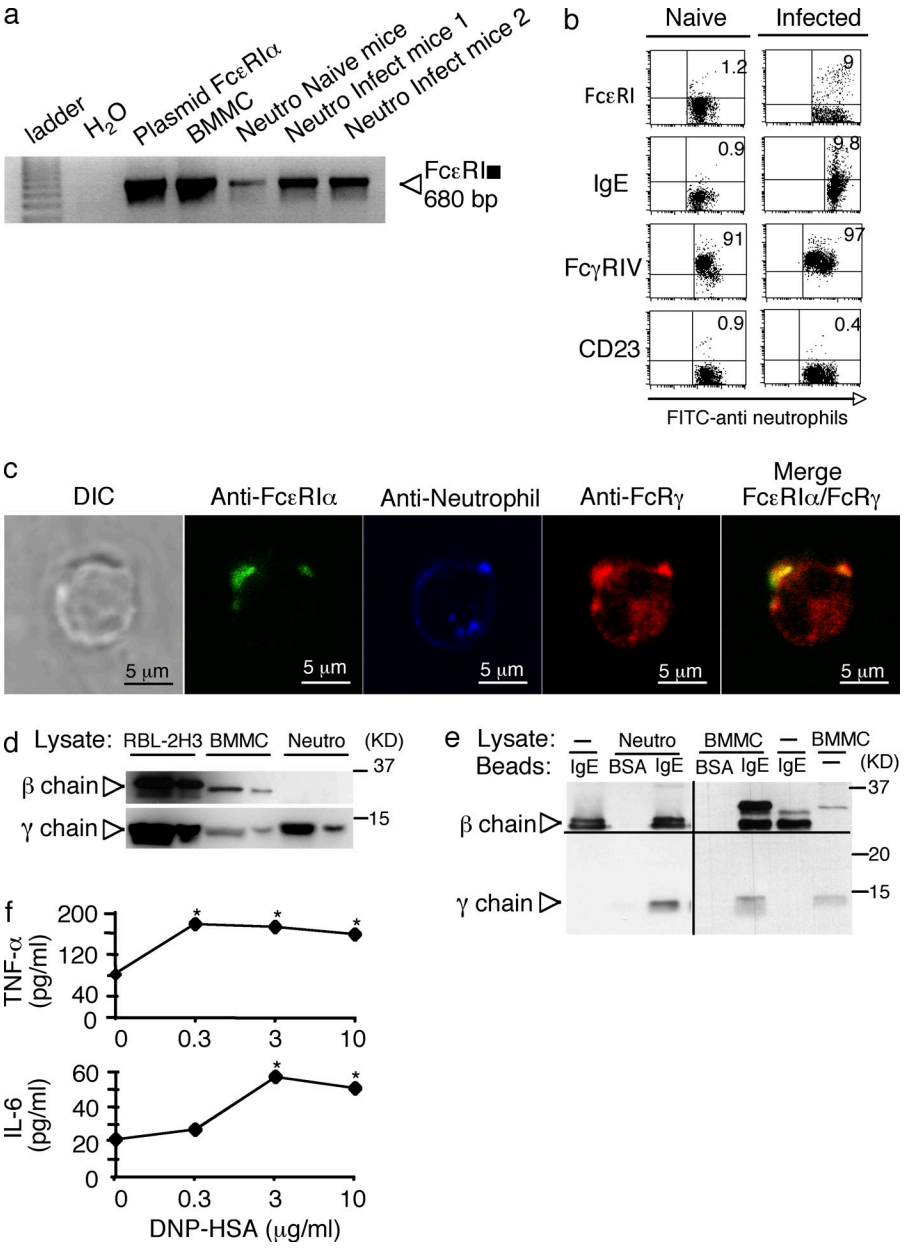

Figure 6. Parasite-induced neutrophils express an unconventional FcεRI. (a) RT-PCR analysis of expression of FcεRα mRNA in naive and 2 *Pb*ANKA-infected neutrophil preparations. RT-PCR from BMMC and PCR amplification of FcεRα plasmid DNA were used as positive controls. Data were from two independent experiments. (b) Neutrophil population was sorted from BM cells from naive C57BL/6 mice or from mice infected 6 d earlier with 10^6 *Pb*ANKA-iRBC. Cells were counter-stained with either anti-FcεRI, anti-IgE, anti-FcγRIV, or anti-CD23 antibodies and comparison was performed between neutrophils from naive and infected mice. Data were obtained from four independent experiments. (c) Percoll-enriched and 7/4-FITC-sorted sorted neutrophils (blue pseudocolor) from the BM of *Pb*ANKA-infected C57BL/6 mice were stained with anti-FcεRI (green pseudocolor) before fixation, permeabilization, and staining, with anti-FcεRI γ (red). Cells were visualized by confocal microscopy. The DIC image, single optical sections through individual cells, as well as the merge (green and red fluorescence) are presented. Bars, 5 μm. Quantitative analysis of colocalization of γ chain with FcεRI (red with green) and of FcεRI with γ chain (green with red) were, respectively, 0.48 ± 0.23 and 0.11 ± 0.10 Data were from three independent experiments. (d) Cell lysates (20 and 5 μg, respectively) from RBL-2H3, BMMC, and Ly6G-FITC–sorted neutrophils were migrated on 15% SDS-PAGE and subjected to immunoblotting with anti-β and anti-γ antibodies. (e) Lysates from indicated cells or buffer control were subjected to immunoprecipitation with BSA- or IgE-Sepharose as indicated, followed by immunoblotting with anti-β and anti-γ antibodies. The results shown are representative of three independent experiments. (f) Neutrophils, which were passively sensitized with anti-DNP IgE mAb, were stimulated with indicated concentrations of DNP-HSA, and release of TNF and IL-6 was determined by ELISA. * represents significant differences observed for TNF (Mann-Whitney test, P = 0.033) and IL-6 (Mann-Whitney test, P = 0.0117) as compared with basal levels. Data shown in d-f, were from two independent experiments.

of infected mice. Conventional effector cells expressing FcεRI in mice consist of MCs and basophils. However, our data using MC-deficient mice or antibody-mediated depletion of basophils excluded MCs and basophils as relevant effector cells. To exclude functional overlap between mast cells and basophils, mast cell–deficient mice treated with the anti–basophil-depleting antibody did not result in any protection against ECM. Previously, MCs and MC-derived TNF were shown to protect against ECM (Furuta et al., 2006). This contradictory result may have been influenced by the different MC-deficient W/W^v mouse strain used, which makes the mice anemic, and thus potentially compromised in controlling a parasite infection. It was also puzzling that TNF was protective in this study, although TNF generally enhances disease severity (Grau et al., 1987).

Searching for alternative FcεRI-expressing cell types, we identified neutrophils and eosinophils, and discovered that the former had a disease enhancing. Although FcεRIα is essentially absent in neutrophils in naive mice, FcεRIα becomes induced during *Plasmodium* infection as demonstrated by: RT-PCR analysis, the binding of the α chain–specific MAR-1 antibody, and detection of membrane-bound IgE. Additional characterization showed that the receptor was colocalized with the FcεRIγ subunit that could be coimmunoprecipitated with IgE. In contrast, the FcεRI β chain was undetectable in neutrophils. Although FcγRIV, which is expressed in neutrophils in both naive and infected mice, could potentially bind IgE at high concentration (Hirano et al., 2007; Mancardi et al., 2008), we did not detect significant IgE binding to this receptor. Similarly, another IgE receptor CD23, was not expressed in neutrophils, suggesting that IgE binding to FcεRI was specific. In humans, FcεRI is frequently expressed in neutrophils of atopic asthmatics as a trimeric FcεRIαγ$_2$ receptor (Saffar et al., 2007), whereas it is absent in healthy individuals. It has therefore been postulated that FcεRI-induced inflammatory signaling and the reported antiapoptotic effect of monomeric IgE may exacerbate the pathogenetic effects of FcεRI$^+$ neutrophils in asthma (Saffar et al., 2007). A parallel can be made in the present work as to the possible implication of FcεRI$^+$ neutrophils in malaria pathogenesis. Indeed, cell type–specific depletion of neutrophils, but not of eosinophils was found to protect mice against ECM and mortality consistent with previous findings using the same neutrophil-depleting antibody (NIMP-R14; Senaldi et al., 1994). Furthermore, transfer of FcεRI$^+$, but not FcεRI$^-$, neutrophils conferred ECM susceptibility to the otherwise resistant FcεRI-α-KO mice. Likewise, irradiated C57BL/6 mice engrafted with the BM from FcεRI-α-KO mice acquired resistance to ECM, which was not the case when these mice were reconstituted with the BM from C57BL/6 mice (unpublished data). These results emphasize the critical role of FcεRI$^+$ neutrophils in the disease expression and mortality, as the sequestration properties of this cell population in the brain tissue occurs rapidly, within an hour after cell transfer, in *Pb*ANKA-infected FcεRI-α-KO mice that are otherwise CM resistant. The fact that the FcεRI$^+$ neutrophils did not sequester in the brain of noninfected mice suggests that the brain tissue of *Pb*ANKA-infected FcεRI-α-KO mice acquired the potential to recruit FcεRI$^+$ neutrophils. After infection, given the absence of FcεRI in these mice, the pathogenetic effects could not be observed. A subsequent issue relates to the specific induction of FcεRI$^+$ neutrophils by the *Pb*ANKA strain, as this cell population was absent when the non–CM-inducing *Pb*NK65 strain was used. Indeed, it is frequently asked what distinguishes these two parasite strains in terms of their ability to cause ECM or not. One possible explanation is provided by the present work, which establishes a close relationship between the disease-associated FcεRI$^+$ neutrophils and CM-inducing *Pb*ANKA strain. However, it remains to be determined at the molecular level by which mechanism *Pb*ANKA induces the expression of FcεRI.

Collectively, our findings provide a new concept on inflammatory response-driven malaria pathogenesis where neutrophils play a central role in inducing inflammatory responses, reminiscent of the allergic-type reactions implicated in the development of ECM. Inflammatory cytokines IFN-γ and IL-6, which have elevated expression locally in the brain and systemically in the plasma, may represent surrogate markers for this neutrophil-mediated response. Because ECM pathology was found to be associated with increased pro-inflammatory IFN-γ (Hunt and Grau, 2003), an attenuated production of this cytokine in FcεRI-α-KO mice raises the possibility that FcεRI$^+$ neutrophils that sequester in the brain of infected C57BL/6 mice may represent an additional source of IFN-γ. Functional studies of FcεRI$^+$ neutrophils via cross-linking of bound IgE results in the production of IL-6 and TNF. In infected mice, the triggering of cytokine release may occur in different tissues, including BM, blood, and brain, giving rise to both systemic and local cytokine induction. Physiologically, several possibilities exist to explain the elevated cytokine levels, such as the possibility that cytokines are released by activated neutrophils subsequent to aggregation of specific IgE antibodies on sensitized neutrophils by parasite-derived antigens. However, this mechanism is uncertain, as we were not able to detect such specific IgE antibodies in infected mice. It is also possible that IgE present in the mouse before infection exerts a priming function when binding to newly expressed FcεRI on a subset of neutrophils, rendering them more responsive to other stimuli.

Several questions remain unresolved. In particular, as mentioned above, the *Plasmodium* infection-associated signals required for the induction of FcεRI expression in neutrophils are unknown. However, this property seems to be specific to the ECM-inducing *Pb*ANKA parasite, as mice infected with non–ECM-inducing *Pb*NK65 parasite or mice infected with *Escherichia coli* undergoing septic peritonitis as a result of cecal ligation and puncture did not show any expression of FcεRI in their neutrophils (unpublished data). In humans, it is believed that expression of FcεRI in neutrophils is regulated by Th2 cytokines (Saffar et al., 2007) and GM-CSF. We detected IL-4 in the brain and in the spleen at 6 d after

infection (unpublished data), but a clear relationship with the induction of IgE and FcεRI$^+$ neutrophils during *Plasmodium* infection was not formally established. Although IgE-KO mice were clinically resistant, our attempts to detect *Plasmodium* antigen-specific IgE antibodies in the plasma of infected mice have failed. It is possible that within the relatively short period of infection (6–8 d), an effective IgE antibody response may be hardly detectable. A significant increase in total IgE antibodies became detectable in surviving mice only at day 12 after infection (Fig. 1 e). One possibility is that limited amounts of IgE antibodies are sufficient to trigger neutrophil responses. Alternatively, sensitization with parasite antigen-unrelated IgE antibodies may render FcεRI$^+$ neutrophils more prone to fulfill their effector functions. In support of this, an earlier study of MCs highlighted the role of antigen-irrelevant IgE in positively influencing hapten-specific contact hypersensitivity (Bryce et al., 2004). Therefore, it is possible that IgE present in the mouse before infection binds to newly expressed FcεRI thereby priming these cells for enhanced effector responses.

Our biochemical analysis showed that mouse neutrophils, express FcεRIαγ_2 trimers in the absence of the β chain (Wang et al., 1992; Maurer et al., 1996). This was surprising, as previous experiments had indicated a requirement of this subunit for cell surface expression in rodents in contrast to the human receptor (Miller et al., 1989), where expression can be observed in several β-less cell types (Bieber, 2007). However, a precedent for the expression of FcεRI in the absence of FcεRIβ in mice has previously been made in lung DCs after infection with Sendai virus (Grayson et al., 2007). It is therefore conceivable that infectious events may enable expression of a trimeric FcεRIαγ_2 receptor by masking inherent retention signals of the α chain (Blank et al., 1991; Hartman et al., 2008). Alternatively, they may induce expression of "β-like" molecules that support receptor expression. Additional studies are necessary to clarify the various aspects leading to the activation of FcεRI$^+$ neutrophils during malaria disease.

Collectively, our data provide evidence for the implication of an unconventional FcεRI in neutrophils as being important in the expression of severe malaria mediated by an IgE-mediated inflammatory response.

MATERIALS AND METHODS

Mice. Female C57BL/6 mice 6–8 wk old were purchased from Charles River Breeding Laboratories. FcεRIα-KO mice have been previously described (Dombrowicz et al., 1993a). IgE single-KO mice were derived from double IgE/CD16-KO mice by backcrosses on C57BL/6 mice (provided by J.S Verbeek, Leiden University Medical Center, Leiden, the Netherlands). These mice were originally provided by H. Oettgen (Children's Hospital, Harvard Medical School, Boston, MA) C57BL/6-*KitW-sh/W-sh* mice were provided by P. Besmer (Sloan-Kettering Institute, New York, NY). All mice were on the C57BL/6 background. All animal care and experimentation was conducted in accordance with the Institut Pasteur animal care and use committee guidelines.

Parasites and infection. For all infections, non–ECM-inducing *P. berghei* (strain NK65; *Pb*NK65) or ECM-inducing (ANKA strain) strains expressing the GFP on CS or hsp70 promoter (Ishino et al., 2006), were used allowing the detection of sporozoites and blood stage parasites by fluorescent microscopy. Parasites were provided by Dr. T. Ishino (Department of Medical Zoology, Mie University School of Medicine, Edobashi, Tsu, Japan). Infection of mice with *Pb*ANKA induces ECM, characterized by paralysis, ataxia, convulsions, and coma between 7–9 d after infection. *Pb*NK65 induces a lethal malaria around 20–25 d after infection without neurological symptoms and was a gift from R. Menard (Institut Pasteur, Paris, France). The parasites were maintained in a cycle between C57BL/6 mice and *Anopheles stephensi* (Demeure et al., 2005). The erythrocytic stages of the parasites were maintained in liquid nitrogen as iRBC in Alsever's solution (Sigma-Aldrich) containing 10% glycerol. The infection is induced either by exposure to 8–10 infected *An. stephensi* mosquitoes (Beghdadi et al., 2008) or by intraperitoneal injection of 10^6 iRBCs.

Flow cytometry analysis. Single-cell suspensions from blood or BM obtained at different time points after inoculation of C57BL/6N mice with 10^6 *Pb*ANKA-iRBCs were stained for FACS analysis according to standard protocols in cold PBS containing 2% FCS and 0.01% sodium azide (FACS buffer). Labeling was performed as follows: for total neutrophils (PerCP-anti-CD45$^+$ FITC-7/4$^+$ PE-anti-Ly6G mAbs), total eosinophils (PerCP-anti-CD45 mAb$^+$ PE-anti-Siglec-F mAb), and total FcεRIα$^+$ leukocytes (PerCP-anti-CD45 mAb + PE-anti-FcεRIα chain mAb). To unequivocally define FcεRI$^+$ neutrophil subpopulation by FACS analyses, cells were labeled with PerCP-antiCD45 mAb and counter-stained with antineutrophil FITC-7/4 and PE-anti-Ly6G antibodies, and with APC-anti-FcεRIα chain mAb. Detection of basophils consisted of PerCP-anti-CD45 mAb + APC-Dx5 + PE-anti-FcεRIα chain mAb). FcεRIα$^+$ eosinophils were identified using PerCP-anti-CD45 mAb + PE-anti-Siglec F mAb + FITC-anti-FcεRIα chain mAb, and mast cells were characterized using PerCP-antiCD45 + APC-anti-CD117 + PE-anti-FcεRIα chain mAbs. All antibodies were obtained from BD, except FITC-7/4 and anti-FcεRIα chain mAbs (clone MAR-1), which were obtained from Invitrogen and eBioscience, respectively. The hamster anti–mouse FcγRIV antibody (clone 9e9) was provided by J. Ravetch (The Rockefeller University, New York, NY). Analysis was performed using a four-color FACSCalibur flow cytometer with ProCellQuest software (BD). Data were expressed as the percentage of total CD45$^+$ BM or blood cells, or as the percentage of total FcεRIα$^+$ BM or blood cells.

Confocal microscopy and immunoprecipitation studies. For confocal immunofluorescence microscopy, FITC-anti-Ly6G$^+$ neutrophils, FcεRI-expressing cells (~0.5×10^6 cells) sorted out by FACS were first incubated with anti-FcεRI antibody MAR-1 (1 h on ice), followed by incubation with Dylight 649 goat anti–Armenian hamster (BioLegend) before fixation for 15 min in PBS containing 4% paraformaldehyde followed by 2 washes in PBS. Fixed cells were permeabilized in PBS containing 0.025% saponin for 20 min at room temperature, followed by blocking in PBS containing 0.025% saponin and 10% goat serum/0.2% BSA (Invitrogen) for 30 min at room temperature. Cells were then stained with rabbit ant-FcRγ in PBS containing 0.025% saponin and 10% goat serum/0.2% BSA overnight at 4°C, followed by incubation with anti–rabbit-Alexa Fluor 568 for 60 min in PBS containing 0.012% saponin and 10% goat serum/0.2% BSA. After washing, cells were mounted in Prolong-Gold anti-fading reagent (Invitrogen) and analyzed using a confocal laser-scanning microscope (LSM 510; Carl Zeiss, Inc.). Images were taken using 63× oil immersion objective lens. Colocalization was quantified using LSM 510 image software. A total of 7 cells with a minimum of 10 stacks were quantified.

Immunoprecipitation and immunoblotting. Ly6G-FITC–sorted positive neutrophils enriched for FcεRI-expressing cells by Percoll gradient centrifugation were washed 2 times in PBS and resuspended at 1×10^6 cells/ml in PBS. 3 million cells were used for preparation of cell lysates in 50 mM Hepes, pH 7.3, containing 0.5% Triton X-100, 150 mM NaCl, 10 mM $MgCL_2$, 50 mM NaF, 1 mM sodium orthovanadate, and the protease inhibitors aprotinin 1,000 U/ml (Sigma-Aldrich), pepstatin 10 μg/ml, leupeptin 20 μg/ml, and AEBSF 2 μM

(Alexis, Inc.). For immunoprecipitation, cells were lysed on ice for 30 min in 50 mM Hepes, pH 7.3, containing 0.3% Triton X-100, 150 mM NaCl, 10 mM $MgCL_2$, 50 mM NaF, 1 mM sodium orthovanadate, and the protease inhibitors aprotinin 1000 U/ml (Sigma-Aldrich), pepstatin 10 µg/ml, leupeptin 20 µg/ml, and AEBSF 2 µM (Alexis, Inc.). After centrifugation, proteins were resolved on SDS-PAGE and transferred onto PVDF membranes (Sigma-Aldrich). Membranes were blocked with 4% BSA for 1 h, followed by incubation with primary mouse anti-FcεRIβ, or rabbit anti-FcεRIγ (1 h at room temperature). After several washes, blots were incubated with goat anti–mouse IgG HRP (1/10,000) or donkey anti–rabbit IgG HRP (Jackson ImmunoResearch Laboratories) for 45 min and were developed by ECL (GE Healthcare).

Real-time RT-PCR and RT-PCR of the α chain of the FcεRI. Gene expression in the brains from FcεRI-α-KO and C57BL/6 mice at various time points after infection were analyzed by the real-time RT-PCR. RNA used for these assays was isolated by means of a two-step extraction process. First, brains were surgically removed from mice as previously described and placed immediately in RNAlater (QIAGEN) at 4°C overnight. After RNAlater infused the samples, it was removed and samples were maintained at −80°C until processing. Brains were thawed in 1 ml of TRIzol and subjected to bead disruption in a polytron 3 times for 2 min at a setting of 30 cycles/s. Samples are spun at high speed (10,000 *g*) for 3 min to remove debris and lipids. Half of the sample was transferred to a new tube and mixed with 500 µl of TRIzol reagent by vortexing. After this step, RNA extraction proceeded according to the manufacturer's protocol. Precipitated mRNA was resuspended in 100 µl of RNase-free water. The second step of this extraction was followed by QIAGEN's protocol for RNA clean-up, including steps for removal of protein and DNA (RNeasy kit; QIAGEN). Samples were eluted with 50 µl of RNase-free water and quality and quantity assured by photospectroscopy. Real-time RT-PCR used primer-probe sets for the α chain of mouse FcεRI and standard TaqMan protocols (Applied Biosystems).

RT-PCR to amplify FcεRIα was performed according to standard procedures as previously described (Roa et al., 1997). 1 µg of mRNA from BMMC, naive, and *Plasmodium*-infected neutrophils were reverse transcribed using Superscript RT (Invitrogen). An aliquot of the cDNA (1 µg) was amplified using primers yielding full-length (680 bp) FcεRIα (5′-ACTGATGAATTCGCCACTGAGAAATCTGTA-3′ and 5′-CTGATAAGCTTGGTTAGGAGTTCGGTTTC-3′) with an annealing temperature of 53°C and 35 cycles of amplification. PCR amplification of FcεRα cDNA (Ra et al., 1991) was used as a positive control.

Detection of IgE antibodies in sera from *Plasmodium*-infected mice. For parasite-specific IgE antibodies, 96-well plates were coated with *Pb*ANKA freeze-thawed crude lysate in carbonate buffer, pH 9.6, for 2 h at 37°C. After the plates were saturated with 1% bovine serum albumin, each serum was assayed at serial dilutions and incubated overnight at 4°C. Specific binding was detected using biotin-conjugated anti–mouse IgE antibodies (BD) followed by streptavidin-alkaline phosphatase (Mabtech) and pNPP as substrate (Sigma-Aldrich).

To determine total IgE, 96-well plates were coated with rat anti–mouse IgE (clone R35-72; BD) for 2 h at 37°C, and the wells were blocked with 1% BSA for 2 h at 37°C. Serial dilutions of sera were incubated overnight at 4°C and developed using biotinylated rat anti–mouse IgE (ε-specific, clone LO-ME-2; Biosys) and streptavidin-alkaline phosphatase (Mabtech). A standard curve was obtained using purified mouse IgE (BD).

Preparation of BM-derived mast cells (BMMCs) and mast cell reconstitution. C57BL/6-*Kit*$^{W\text{-}sh/W\text{-}sh}$ (*W*^{sh}) mice are now used in many instances as a model for studies of mast cell function in vivo (Mallen-St. Clair et al., 2004). *W-sash* (*W*^{sh}) is an inversion mutation in the transcriptional regulatory elements upstream of the *c-kit* transcription start site on mouse chromosome 5 (Nagle et al., 1995). This mutation results in the lack of differentiation of mast cells. *Kit*$^{W\text{-}sh/W\text{-}sh}$ and FcεRIα-KO mice can be transplanted successfully with BM-derived mast cells by injecting 5×10^6 cultured BMMC intraperitoneally.

BMMCs were prepared as previously described (Razin et al., 1981). After 3 wk of culture of BM cells using RPMI 1640 (BioWhittaker) supplemented with 10% heat-inactivated FCS (Boehringer Mannhein) and 3 U/ml of rIL-3, the cells were harvested. They consisted of 98% pure mast cell populations as assessed by toluidine blue staining, and c-Kit and FcεRI expression.

Adoptive transfer. Adoptive transfer experiments were performed by injecting BM cells from C57BL/6 mice into irradiated FcεRIα-KO mice. The reverse adoptive transfer, which consists of the transplantation of BM cells from FcεRIα-KO mice into irradiated C57BL/6 mice was also performed. FcεRIα-KO mice received myeloablative total-body irradiation (900 cGy; ^{137}Cs source), followed by i.v. injection of 5×10^6 donor BM cells from autologous or C57BL/6 WT mice. BM cell suspensions were prepared by flushing femurs with RPMI 1640 medium supplemented with 10% FCS, nonessential amino acids, L-glutamine, sodium pyruvate, and 2-mercaptoethanol. 6 wk after irradiation, chimeric and control mice were infected as described.

For short-term reconstitutions with neutrophils, BM cell suspensions, obtained from *Pb*ANKA-infected C57BL/6 mice (6 d after infection) were separated over a discontinuous density Percoll gradient as indicated in Fig. S3. Each fraction was labeled with FITC-antineutrophils (clone 7/4), PE-anti-Ly6G, and APC-anti FcεRI antibodies (clone MAR-1). The Percoll density layers corresponding to 50 and 45% were found to be enriched in FcεRI$^+$ neutrophil population and were considered for cell sorting. Double-positive cells gated on 7/4 and Ly6G expression isolated from *Pb*ANKA-infected mice gave rise to two neutrophil populations: Ly6G$^+$ 7/4$^+$ FcεRI$^+$ and Ly6G$^+$ 7/4$^+$ FcεRI$^-$ neutrophils (Fig. S4). Sorted triple-positive (Ly6G$^+$ 7/4$^+$ FcεRI$^+$) neutrophils and the double-positive (Ly6G$^+$ 7/4$^+$ FcεRI$^-$) neutrophils (2×10^6 neutrophils/mouse) were injected intravenously in recipient FcεRIα-KO mice. Given the short half-life of neutrophils, their injection at day 6 after infection was taken as the optimal proximal time before the manifestation of disease signs.

Neutrophil activation and cytokine release. Purified neutrophils were resuspended at 10^6 cells/ml in RPMI-1640 medium supplemented with 10% (vol/vol) fetal bovine serum, 2 mM L-glutamine, 100 U/ml penicillin, and 100 mg/ml streptomycin, and then incubated for 1 h with 1 µg/ml of anti-dinitrophenyl (DNP)-specific IgE mAb obtained from culture media of the hybridoma Hi-DNP-ε-26.82 (Liu et al., 1980). For stimulation, the cells were incubated with DNP-HSA at 37°C for indicated times. Supernatants were then tested for IL-6 and TNF content by ELISA (BD). Lysates were tested for phosphorylation of p38 MAPK and Akt.

In vivo depletion of basophils, neutrophils, and eosinophils. Basophils represent <1% of peripheral blood leukocytes and have been neglected until recently, when they were found to fulfill critical immunological functions (Karasuyama et al., 2009). These cells, which generate large quantities of T helper 2 (Th2) cytokines such as IL-4, provided new insights into their possible role in allergic disorders and immunity to pathogens. A specific antibody has recently been generated, the rat monoclonal antibody Ba103, which recognizes a mouse basophil-associated protein (Obata et al., 2007). For basophil depletion, mice were given an intravenous injection of Ba103 1 d before infection with 10^6 RBCs. A single intravenous administration of 30 µg Ba103 drastically reduced the basophil number in the peripheral blood, and this level remained reduced for ∼10 d after the single injection of Ba103, and thereafter returned to normal. Unlike the number of basophils, no significant reduction in the number of mast cells was observed (Obata et al., 2007). To determine if eosinophils and neutrophils play any role in malaria disease severity, cell-specific depletion experiments were performed. C57BL/6 mice were injected 1 d before infection with *Pb*ANKA pRBCs, with 200 µg of a rat anti–mouse neutrophils (clone NIMP-R14; Senaldi et al., 1994) provided by G. Milon (Institut Pasteur, Paris), which was shown to recognize the same neutrophil population as the anti-Ly6G and the 7/4 mAbs, or with 100 µg of an affinity purified polyclonal antibody raised in sheep against Siglec-F, a specific marker for mouse eosinophils, which was obtained from P. Crocker (Division of Cell Biology and Immunology, The Wellcome Trust Biocentre at Dundee,

University of Dundee, UK; Zimmermann et al., 2008). A second injection of anti-Siglec-F antibody was provided at day 4 after infection to maintain eosinophils at a minimal level until the expression of clinical signs. At day 6, when the first clinical signs appear, no detectable neutrophils or eosinophils were present in peripheral blood. To verify if NIMP-R14 antibody specifically recognizes neutrophil cells, BM cells obtained 6 d after infection from C57BL/6 mice were first stained with NIMP-R14 mAb followed by anti-rat IgG mAb-PE/Cy7 and positive cells were sorted out. NIMP-R14$^+$ cells were then counter-stained with anti-GR-1-PE, 7/4-FITC, MAR-1-Alexa Fluor 647, CD11c-PE, DX5-PE, F4/80-PE, CD11b-FITC, and Siglec-F-PE antibodies. The pattern of stainings shows a complete overlap between the NIPM-R14 antibody and the anti-Ly6G and 7/4 antibodies.

Statistical analysis. Significant differences in survival were evaluated by generation of Kaplan-Meier plots and log rank analysis. $P < 0.05$ was considered statistically significant. For other analyses, after verification using a Jarque-Bera test, our data followed a normal distribution; statistical significance was assessed by an ANOVA test followed by an *a posteriori* Fisher PLSD (Protected Least Significant Difference) test. For parasitemia, after verification using a Jarque-Bera test, our data did not follow normal distribution, and thus, when differences between groups of mice were to be compared at a given time point, the Mann-Whitney test was performed with significance set at $P < 0.05$.

Online supplemental material. Fig. S1 shows an assessment of mast cell development and function in FcεRIα-KO mice and mast cell reconstitution of FcεRIα-KO mice and Wsh mice. Fig. S2 shows in vivo depletion of basophils. Fig. S3 shows density-based distribution of FcεRI$^+$ neutrophils. Fig. S4 shows the phenotypic characterization of FcεRI$^+$ neutrophils. Online supplemental material is available at http://www.jem.org/cgi/content/full/jem.20110845/DC1.

We thank Jeffrey V. Ravetch (The Rockefeller University) and Paul Crocker (University of Dundee) for providing anti-mouse FcγRIV and anti-Siglec-F antibodies, respectively. We also thank Hans Oettgen (Children's Hospital, Harvard Medical School) and Sjef J. Verbeek (Leiden University Medical Center) for providing IgE-KO mice. We thank CEPIA (Centre d'élevage, de production et d'infection des anopheles, Institut Pasteur) for providing anopheles mosquitoes. We thank Karine Ronce for her technical assistance.

The authors declare no competing financial interests.

Author contributions A. Porcherie, C. Mathieu, R. Peronet, and U. Blank performed experiments and analyzed the data. H. Kiefer-Biasizzo, and J. Claver gave technical support. G. Milon, H. Karasuyama, M. Dy, J.-P. Kinet, and J. Louis developed analytical tools and gave conceptual advice. U. Blank and S. Mécheri wrote the paper. S. Mécheri conceived the study. All authors discussed the results and commented the manuscript at all stages.

Submitted: 28 April 2011
Accepted: 29 August 2011

REFERENCES

Beghdadi, W., A. Porcherie, B.S. Schneider, D. Dubayle, R. Peronet, M. Huerre, T. Watanabe, H. Ohtsu, J. Louis, and S. Mécheri. 2008. Inhibition of histamine-mediated signaling confers significant protection against severe malaria in mouse models of disease. *J. Exp. Med.* 205:395–408. http://dx.doi.org/10.1084/jem.20071548

Bereczky, S., S.M. Montgomery, M. Troye-Blomberg, I. Rooth, M.A. Shaw, and A. Färnert. 2004. Elevated anti-malarial IgE in asymptomatic individuals is associated with reduced risk for subsequent clinical malaria. *Int. J. Parasitol.* 34:935–942. http://dx.doi.org/10.1016/j.ijpara.2004.04.007

Bhattacharya, U., S. Roy, P.K. Kar, B. Sarangi, and S.C. Lahiri. 1988. Histamine & kinin system in experimental malaria. *Indian J. Med. Res.* 88:558–563.

Bieber, T. 2007. The pro- and anti-inflammatory properties of human antigen-presenting cells expressing the high affinity receptor for IgE (Fc epsilon RI). *Immunobiology.* 212:499–503. http://dx.doi.org/10.1016/j.imbio.2007.03.001

Blank, U., and J. Rivera. 2004. The ins and outs of IgE-dependent mast-cell exocytosis. *Trends Immunol.* 25:266–273. http://dx.doi.org/10.1016/j.it.2004.03.005

Blank, U., C.S. Ra, and J.P. Kinet. 1991. Characterization of truncated alpha chain products from human, rat, and mouse high affinity receptor for immunoglobulin E. *J. Biol. Chem.* 266:2639–2646.

Bryce, P.J., M.L. Miller, I. Miyajima, M. Tsai, S.J. Galli, and H.C. Oettgen. 2004. Immune sensitization in the skin is enhanced by antigen-independent effects of IgE. *Immunity.* 20:381–392. http://dx.doi.org/10.1016/S1074-7613(04)00080-9

Coban, C., K.J. Ishii, T. Kawai, H. Hemmi, S. Sato, S. Uematsu, M. Yamamoto, O. Takeuchi, S. Itagaki, N. Kumar, et al. 2005. Toll-like receptor 9 mediates innate immune activation by the malaria pigment hemozoin. *J. Exp. Med.* 201:19–25. http://dx.doi.org/10.1084/jem.20041836

Coban, C., K.J. Ishii, S. Uematsu, N. Arisue, S. Sato, M. Yamamoto, T. Kawai, O. Takeuchi, H. Hisaeda, T. Horii, and S. Akira. 2007. Pathological role of Toll-like receptor signaling in cerebral malaria. *Int. Immunol.* 19:67–79. http://dx.doi.org/10.1093/intimm/dxl123

Demeure, C.E., K. Brahimi, F. Hacini, F. Marchand, R. Péronet, M. Huerre, P. St-Mezard, J.F. Nicolas, P. Brey, G. Delespesse, and S. Mécheri. 2005. Anopheles mosquito bites activate cutaneous mast cells leading to a local inflammatory response and lymph node hyperplasia. *J. Immunol.* 174:3932–3940.

Dombrowicz, D., V. Flamand, K.K. Brigman, B.H. Koller, and J.P. Kinet. 1993a. Abolition of anaphylaxis by targeted disruption of the high affinity immunoglobulin E receptor alpha chain gene. *Cell.* 75:969–976. http://dx.doi.org/10.1016/0092-8674(93)90540-7

Dombrowicz, D., V. Flamand, K.K. Brigman, B.H. Koller, and J.P. Kinet. 1993b. Abolition of anaphylaxis by targeted disruption of the high affinity immunoglobulin E receptor alpha chain gene. *Cell.* 75:969–976. http://dx.doi.org/10.1016/0092-8674(93)90540-7

Furuta, T., T. Kikuchi, Y. Iwakura, and N. Watanabe. 2006. Protective roles of mast cells and mast cell-derived TNF in murine malaria. *J. Immunol.* 177:3294–3302.

Ganguly, S., C. Grodzki, D. Sugden, M. Møller, S. Odom, P. Gaildrat, I. Gery, R.P. Siraganian, J. Rivera, and D.C. Klein. 2007. Neural adrenergic/cyclic AMP regulation of the immunoglobulin E receptor alpha-subunit expression in the mammalian pinealocyte: a neuroendocrine/immune response link? *J. Biol. Chem.* 282:32758–32764. http://dx.doi.org/10.1074/jbc.M705950200

Grau, G.E., and S. de Kossodo. 1994. Cerebral malaria: mediators, mechanical obstruction or more? *Parasitol. Today (Regul. Ed.).* 10:408–409. http://dx.doi.org/10.1016/0169-4758(94)90236-4

Grau, G.E., L.F. Fajardo, P.F. Piguet, B. Allet, P.H. Lambert, and P. Vassalli. 1987. Tumor necrosis factor (cachectin) as an essential mediator in murine cerebral malaria. *Science.* 237:1210–1212. http://dx.doi.org/10.1126/science.3306918

Grau, G.E., T.E. Taylor, M.E. Molyneux, J.J. Wirima, P. Vassalli, M. Hommel, and P.H. Lambert. 1989. Tumor necrosis factor and disease severity in children with falciparum malaria. *N. Engl. J. Med.* 320:1586–1591. http://dx.doi.org/10.1056/NEJM198906153202404

Grayson, M.H., D. Cheung, M.M. Rohlfing, R. Kitchens, D.E. Spiegel, J. Tucker, J.T. Battaile, Y. Alevy, L. Yan, E. Agapov, et al. 2007. Induction of high-affinity IgE receptor on lung dendritic cells during viral infection leads to mucous cell metaplasia. *J. Exp. Med.* 204:2759–2769. http://dx.doi.org/10.1084/jem.20070360

Hartman, M.L., S.Y. Lin, M.H. Jouvin, and J.P. Kinet. 2008. Role of the extracellular domain of Fc epsilon RI alpha in intracellular processing and surface expression of the high affinity receptor for IgE Fc epsilon RI. *Mol. Immunol.* 45:2307–2311. http://dx.doi.org/10.1016/j.molimm.2007.11.017

Hirano, M., R.S. Davis, W.D. Fine, S. Nakamura, K. Shimizu, H. Yagi, K. Kato, R.P. Stephan, and M.D. Cooper. 2007. IgEb immune complexes activate macrophages through FcgammaRIV binding. *Nat. Immunol.* 8:762–771. http://dx.doi.org/10.1038/ni1477

Hunt, N.H., and G.E. Grau. 2003. Cytokines: accelerators and brakes in the pathogenesis of cerebral malaria. *Trends Immunol.* 24:491–499. http://dx.doi.org/10.1016/S1471-4906(03)00229-1

Ishino, T., Y. Orito, Y. Chinzei, and M. Yuda. 2006. A calcium-dependent protein kinase regulates Plasmodium ookinete access to the midgut epithelial cell. *Mol. Microbiol.* 59:1175–1184. http://dx.doi.org/10.1111/j.1365-2958.2005.05014.x

Karasuyama, H., K. Mukai, Y. Tsujimura, and K. Obata. 2009. Newly discovered roles for basophils: a neglected minority gains new respect. *Nat. Rev. Immunol.* 9:9–13. http://dx.doi.org/10.1038/nri2458

Kwiatkowski, D. 1995. Malarial toxins and the regulation of parasite density. *Parasitol. Today (Regul. Ed.).* 11:206–212. http://dx.doi.org/10.1016/0169-4758(95)80079-4

Kwiatkowski, D., A.V. Hill, I. Sambou, P. Twumasi, J. Castracane, K.R. Manogue, A. Cerami, D.R. Brewster, and B.M. Greenwood. 1990. TNF concentration in fatal cerebral, non-fatal cerebral, and uncomplicated Plasmodium falciparum malaria. *Lancet.* 336:1201–1204. http://dx.doi.org/10.1016/0140-6736(90)92827-5

Liu, F.T., J.W. Bohn, E.L. Ferry, H. Yamamoto, C.A. Molinaro, L.A. Sherman, N.R. Klinman, and D.H. Katz. 1980. Monoclonal dinitrophenyl-specific murine IgE antibody: preparation, isolation, and characterization. *J. Immunol.* 124:2728–2737.

Lou, J., Y. Gasche, L. Zheng, B. Critico, C. Monso-Hinard, P. Juillard, P. Morel, W.A. Buurman, and G.E. Grau. 1998. Differential reactivity of brain microvascular endothelial cells to TNF reflects the genetic susceptibility to cerebral malaria. *Eur. J. Immunol.* 28:3989–4000.

Mallen-St Clair, J., C.T.N. Pham, S.A. Villalta, G.H. Caughey, and P.J. Wolters. 2004. Mast cell dipeptidyl peptidase I mediates survival from sepsis. *J. Clin. Invest.* 113:628–634.

Mancardi, D.A., B. Iannascoli, S. Hoos, P. England, M. Daëron, and P. Bruhns. 2008. FcgammaRIV is a mouse IgE receptor that resembles macrophage FcepsilonRI in humans and promotes IgE-induced lung inflammation. *J. Clin. Invest.* 118:3738–3750. http://dx.doi.org/10.1172/JCI36452

Maneerat, Y., P. Viriyavejakul, B. Punpoowong, M. Jones, P. Wilairatana, E. Pongponratn, G.D. Turner, and R. Udomsangpetch. 2000. Inducible nitric oxide synthase expression is increased in the brain in fatal cerebral malaria. *Histopathology.* 37:269–277. http://dx.doi.org/10.1046/j.1365-2559.2000.00989.x

Maurer, D., S. Fiebiger, C. Ebner, B. Reininger, G.F. Fischer, S. Wichlas, M.H. Jouvin, M. Schmitt-Egenolf, D. Kraft, J.P. Kinet, and G. Stingl. 1996. Peripheral blood dendritic cells express Fc epsilon RI as a complex composed of Fc epsilon RI alpha- and Fc epsilon RI gamma-chains and can use this receptor for IgE-mediated allergen presentation. *J. Immunol.* 157:607–616.

Metzger, W.G., D.M. Okenu, D.R. Cavanagh, J.V. Robinson, K.A. Bojang, H.A. Weiss, J.S. McBride, B.M. Greenwood, and D.J. Conway. 2003. Serum IgG3 to the Plasmodium falciparum merozoite surface protein 2 is strongly associated with a reduced prospective risk of malaria. *Parasite Immunol.* 25:307–312. http://dx.doi.org/10.1046/j.1365-3024.2003.00636.x

Miller, L., U. Blank, H. Metzger, and J.P. Kinet. 1989. Expression of high-affinity binding of human immunoglobulin E by transfected cells. *Science.* 244:334–337. http://dx.doi.org/10.1126/science.2523561

Nacher, M., F. Gay, P. Singhasivanon, S. Krudsood, S. Treeprasertsuk, D. Mazier, I. Vouldoukis, and S. Looareesuwan. 2000. Ascaris lumbricoides infection is associated with protection from cerebral malaria. *Parasite Immunol.* 22:107–113. http://dx.doi.org/10.1046/j.1365-3024.2000.00284.x

Nagle, D.L., C.A. Kozak, H. Mano, V.M. Chapman, and M. Buc´an. 1995. Physical mapping of the Tec and Gabrb1 loci reveals that the Wsh mutation on mouse chromosome 5 is associated with an inversion. *Hum. Mol. Genet.* 4:2073–2079. http://dx.doi.org/10.1093/hmg/4.11.2073

Nyakeriga, M.A., M. Troye-Blomberg, S. Bereczky, H. Perlmann, P. Perlmann, and G. ElGhazali. 2003. Immunoglobulin E (IgE) containing complexes induce IL-4 production in human basophils: effect on Th1-Th2 balance in malaria. *Acta Trop.* 86:55–62. http://dx.doi.org/10.1016/S0001-706X(03)00005-6

Oakley, M.S., V. Majam, B. Mahajan, N. Gerald, V. Anantharaman, J.M. Ward, L.J. Faucette, T.F. McCutchan, H. Zheng, M. Terabe, et al. 2009. Pathogenic roles of CD14, galectin-3, and OX40 during experimental cerebral malaria in mice. *PLoS ONE.* 4:e6793. http://dx.doi.org/10.1371/journal.pone.0006793

Obata, K., K. Mukai, Y. Tsujimura, K. Ishiwata, Y. Kawano, Y. Minegishi, N. Watanabe, and H. Karasuyama. 2007. Basophils are essential initiators of a novel type of chronic allergic inflammation. *Blood.* 110:913–920. http://dx.doi.org/10.1182/blood-2007-01-068718

Oettgen, H.C., T.R. Martin, A. Wynshaw-Boris, C. Deng, J.M. Drazen, and P. Leder. 1994. Active anaphylaxis in IgE-deficient mice. *Nature.* 370:367–370. http://dx.doi.org/10.1038/370367a0

Perlmann, H., H. Helmby, M. Hagstedt, J. Carlson, P.H. Larsson, M. Troye-Blomberg, and P. Perlmann. 1994. IgE elevation and IgE anti-malarial antibodies in Plasmodium falciparum malaria: association of high IgE levels with cerebral malaria. *Clin. Exp. Immunol.* 97:284–292. http://dx.doi.org/10.1111/j.1365-2249.1994.tb06082.x

Perlmann, P., H. Perlmann, B.W. Flyg, M. Hagstedt, G. Elghazali, S. Worku, V. Fernandez, A.S. Rutta, and M. Troye-Blomberg. 1997. Immunoglobulin E, a pathogenic factor in Plasmodium falciparum malaria. *Infect. Immun.* 65:116–121.

Perlmann, P., H. Perlmann, S. Looareesuwan, S. Krudsood, S. Kano, Y. Matsumoto, G. Brittenham, M. Troye-Blomberg, and M. Aikawa. 2000. Contrasting functions of IgG and IgE antimalarial antibodies in uncomplicated and severe Plasmodium falciparum malaria. *Am. J. Trop. Med. Hyg.* 62:373–377.

Ra, C., M.H. Jouvin, and J.P. Kinet. 1991. Complete structure of the mouse mast cell receptor for IgE (Fc{varepsilon}RI) and surface expression of chimeric receptors (rat-mouse-human) on transfected cells. *J. Biol. Chem.* 264:15323–15327.

Razin, E., C. Cordon-Cardo, and R.A. Good. 1981. Growth of a pure population of mouse mast cells in vitro with conditioned medium derived from concanavalin A-stimulated splenocytes. *Proc. Natl. Acad. Sci. USA.* 78:2559–2561. http://dx.doi.org/10.1073/pnas.78.4.2559

Roa, M., F. Paumet, J. Le Mao, B. David, and U. Blank. 1997. Involvement of the ras-like GTPase rab3d in RBL-2H3 mast cell exocytosis following stimulation via high affinity IgE receptors (Fc epsilonRI). *J. Immunol.* 159:2815–2823.

Saffar, A.S., M.P. Alphonse, L. Shan, K.T. Hayglass, F.E. Simons, and A.S. Gounni. 2007. IgE modulates neutrophil survival in asthma: role of mitochondrial pathway. *J. Immunol.* 178:2535–2541.

Senaldi, G., C. Vesin, R. Chang, G.E. Grau, and P.F. Piguet. 1994. Role of polymorphonuclear neutrophil leukocytes and their integrin CD11a (LFA-1) in the pathogenesis of severe murine malaria. *Infect. Immun.* 62:1144–1149.

Shi, Y.P., U. Sayed, S.H. Qari, J.M. Roberts, V. Udhayakumar, A.J. Oloo, W.A. Hawley, D.C. Kaslow, B.L. Nahlen, and A.A. Lal. 1996. Natural immune response to the C-terminal 19-kilodalton domain of Plasmodium falciparum merozoite surface protein 1. *Infect. Immun.* 64:2716–2723.

Srichaikul, T., N. Archararit, T. Siriasawakul, and T. Viriyapanich. 1976. Histamine changes in Plasmodium falciparum malaria. *Trans. R. Soc. Trop. Med. Hyg.* 70:36–38. http://dx.doi.org/10.1016/0035-9203(76)90004-3

Stevenson, M.M., and E.M. Riley. 2004. Innate immunity to malaria. *Nat. Rev. Immunol.* 4:169–180. http://dx.doi.org/10.1038/nri1311

Wang, B., A. Rieger, O. Kilgus, K. Ochiai, D. Maurer, D. Födinger, J.P. Kinet, and G. Stingl. 1992. Epidermal Langerhans cells from normal human skin bind monomeric IgE via Fc epsilon RI. *J. Exp. Med.* 175:1353–1365. http://dx.doi.org/10.1084/jem.175.5.1353

Zimmermann, N., M.L. McBride, Y. Yamada, S.A. Hudson, C. Jones, K.D. Cromie, P.R. Crocker, M.E. Rothenberg, and B.S. Bochner. 2008. Siglec-F antibody administration to mice selectively reduces blood and tissue eosinophils. *Allergy.* 63:1156–1163. http://dx.doi.org/10.1111/j.1398-9995.2008.01709.x

SUPPLEMENTAL MATERIAL

Porcherie et al., http://www.jem.org/cgi/content/full/jem.20110845/DC1

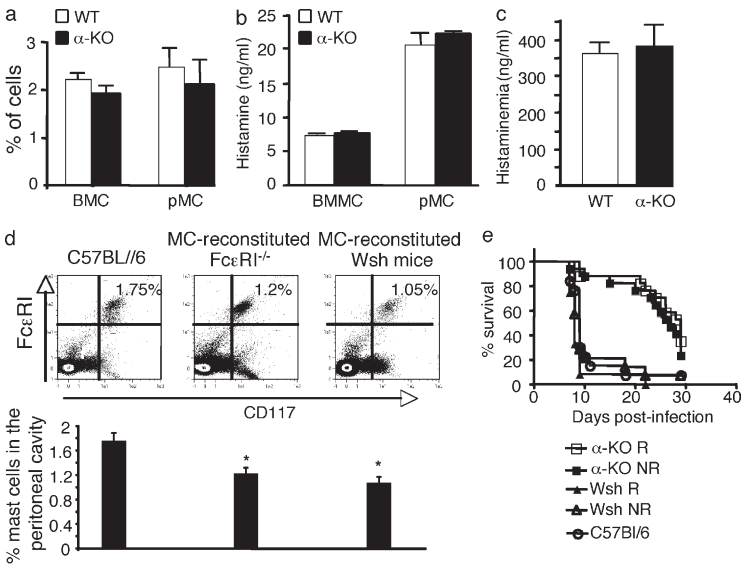

Figure S1. Assessment of mast cell development and function in FcεRIα-KO mice, and of mast cell reconstitution of FcεRIα-KO mice and Wsh mice. (a) BM cells (BMC) and peritoneal MCs (pMC) taken from C57BL/6N (WT) mice and FcεRIα-KO mice were analyzed for the presence of mast cells. Data are expressed as a percentage of total $CD45^+$ cells. (b) Cultured BMMCs and peritoneal cells (5×10^5 cells) obtained from C57BL/6N (WT) or FcεRIα-KO mice, were examined for their histamine content as measured by ELISA. (c) Plasma from C57BL/6N (WT) mice and FcεRIα-KO mice were examined for their histamine content. All analyses gave no significant differences between the two mouse strains. Results were from two independent experiments. (d) FcεRIα-KO mice and W^{sh}/W^{sh} mice were reconstituted with 5×10^6 cultured BMMCs isolated from C57BL/6N (WT) mice. 10 wk after reconstitution, peritoneal cells were analyzed for the presence of $FcεRI^+/CD117^+$ mast cells. Quadrant analysis shows the proportion of MCs in reconstituted FcεRIα-KO and Wsh mice as compared with WT C57BL/6 mice. Data shown are the mean ± SD of 5 reconstituted mice. * indicates significant differences as compared with C57BL/6 mice ($P < 0.03$). Results were from two independent experiments. (e) FcεRIα-KO mice and W^{sh}/W^{sh} mice were reconstituted with 5×10^6 WT BMMCs derived from C57BL/6N (WT) mice. FcεRIα-KO mice (α-KO NR), FcεRIα-KO reconstituted mice (α-KO R), W^{sh}/W^{sh} mice (Wsh NR), W^{sh}/W^{sh} reconstituted mice (Wsh R), and C57BL/6N (WT) mice were infected with *Pb*ANKA via mosquito bites (8–10 mosquitoes per mouse). Kaplan-Meier survival plots were recorded. After an a posteriori test, significant differences in survival/mortality ($n = 12–17$; $P = 0.0006$) were observed between α-KO NR and α-KO R groups and the rest of the groups (median mortality is 27 and 8 d, respectively for the two groups). Data were from two independent experiments.

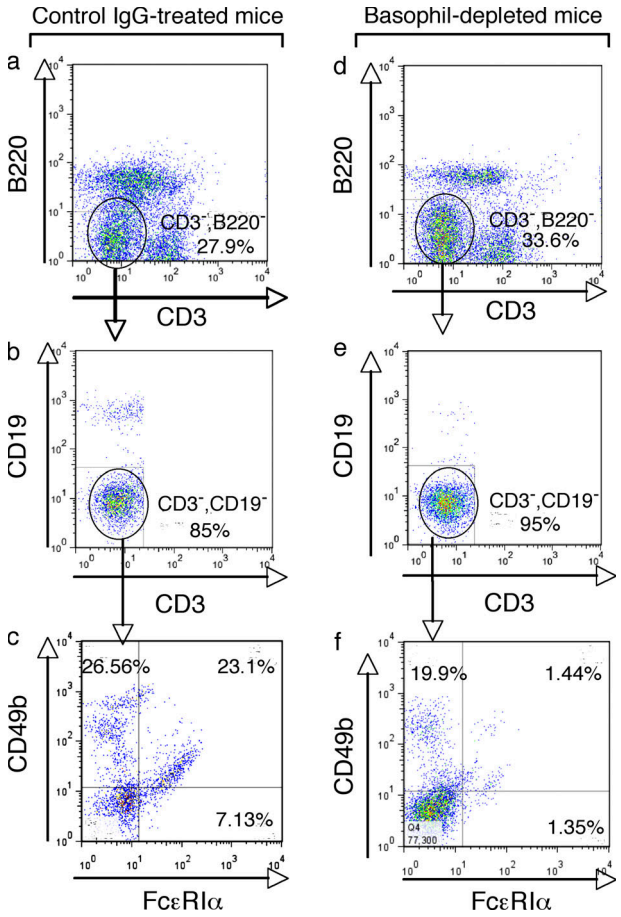

Figure S2. In vivo depletion of basophils. C57BL/6 mice received either 30 µg of the antibasophil antibody Ba103 antibody or control isotype IgG. Blood leukocytes were harvested 48 h later and stained with anti-CD3, anti-B220, anti-CD19, anti-CD49b (DX5), and anti-FcεRI (MAR-1) antibodies. Gated cells on $CD3^-$ $B220^-$ (a and d) and on $CD3^-$ $CD19^-$ non-B non-T cells (b and e) were analyzed for their expression of CD49b and FcεRI (c and f). Data were obtained from one experiment using three independent C57BL/6 mice.

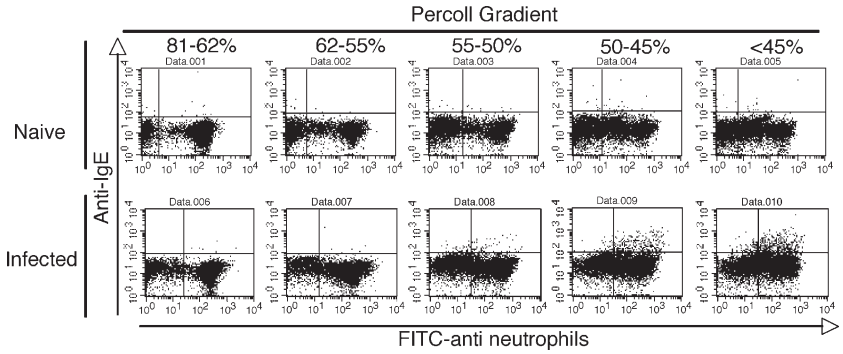

Figure S3. Density-based distribution of FcεRI⁺ neutrophils. BM cell suspensions, obtained from naive and *Pb*ANKA-infected C57BL/6 mice at 6 d after infection were separated over a discontinuous density Percoll gradient, as indicated. Each fraction was labeled with 7/4-FITC-antineutrophils, anti-Ly6G-Alexa Fluor 647, and PE-anti-mouse IgE antibodies. Results are representative of three independent experiments using pooled cells from six C57BL/6 mice.

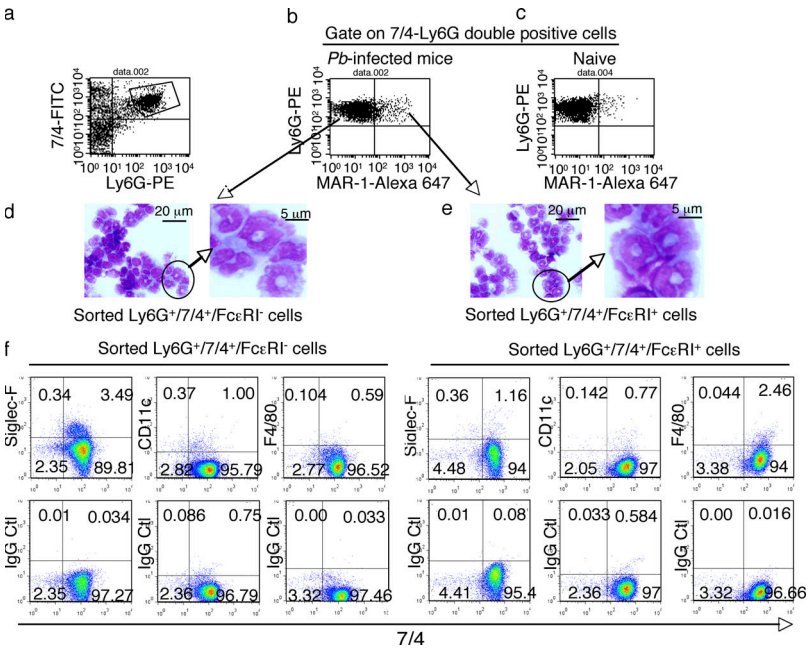

Figure S4. Phenotypic characterization of FcεRI⁺ neutrophils. The Percoll gradient procedure (Fig. S3) was intended to enrich FcεRI⁺ neutrophil population and to increase the efficacy of cell sorting. The cells were labeled with the 7/4-FITC, anti-FcεRI-APC, and anti-Ly6G-PE antibodies. Double-positive cells gated on 7/4 and Ly6G expression (a) isolated from *Pb*ANKA-infected mice gave rise to two neutrophil populations: Ly6G⁺ 7/4⁺ FcεRI⁺ and Ly6G⁺ 7/4⁺ FcεRI⁻ neutrophils (b). Similar analysis was performed on cells from naive mice (c). To further analyze the phenotype of distinct neutrophil populations, sorted Ly6G⁺ 7/4⁺ FcεRI⁻ (d) and Ly6G⁺ 7/4⁺ FcεRI⁺ (e) were subjected to cytospin centrifugation and stained with Giemsa. All neutrophil populations display similar and homogeneous microscopic morphology. Data obtained were from two independent experiments. (B) FACS sorted Ly6G⁺ 7/4⁺ FcεRI⁻ (f) and Ly6G⁺ 7/4⁺ FcεRI⁺ (g) neutrophils were labeled with anti–Siglec-F, anti-CD11c, and anti-F4/80 antibodies for the possible presence of eosinophils, DCs, or macrophages, respectively. Quadrant analysis was performed on 7/4-positive cells labeled with either specific antibodies or with isotype control IgG antibodies. Shown is a representative analysis of two distinct cell preparations.